

# Pancreatic Protection Elicited by Platelet-Rich Plasma and Cinnamon Combination in a Rat Model of Type 1 Diabetes: is it a New Era in Islet Cell Regeneration and Insulin Signalling Genes?

Usama Fouad Ahmed Ebrahim<sup>1</sup>, Ahmed A. Morsi<sup>2</sup>, Hanan Fouad<sup>3</sup> and Eman Mohamed Faruk<sup>4,5</sup>

## Original Article

<sup>1</sup>Department of Anatomy, Faculty of Medicine, Benha University, Egypt

<sup>2</sup>Department of Histology and Cell Biology, Faculty of Medicine, Fayoum University, Fayoum, Egypt

<sup>3</sup>Department of Medical Biochemistry and Molecular Biology, Faculty of Medicine, Cairo University, Cairo, Egypt

<sup>4</sup>Department of Anatomy, Faculty of Medicine, Umm Al-Qura University, Saudi Arabia

<sup>5</sup>Department of Histology and Cytology, Faculty of Medicine, Benha University, Benha, Egypt

## ABSTRACT

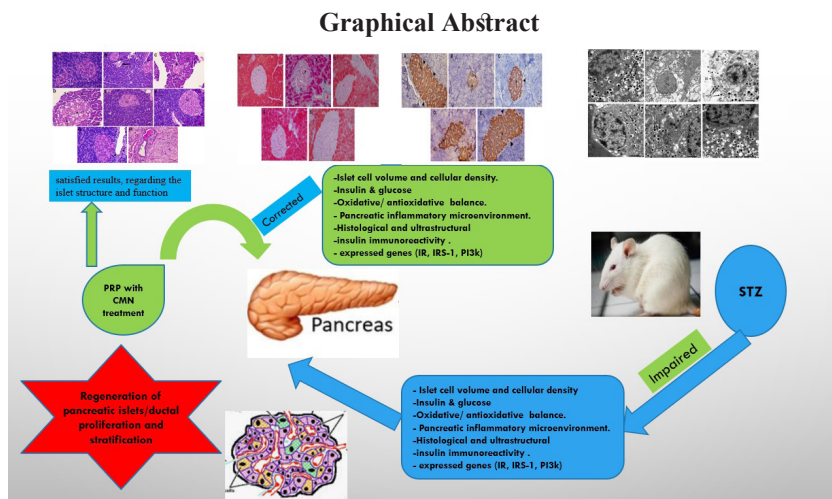
**Introduction:** Enhancement of islet cell regeneration is a great demand that worth the attention of researchers and health-care providers to replace the risk of  $\beta$ -cell transplantation in type 1 diabetic patients.

**Aim:** Evaluation of the regenerative and therapeutic potential of cinnamon (CMN) and platelet-rich plasma (PRP) either alone or combined on the reversal of the pancreatic ultrastructure and insulin signalling pathway in STZ-induced diabetic rats.

**Materials and Methods:** Fifteen adult male albino rats were used for obtaining PRP and the remaining 35 rats were used as control, diabetic (STZ, 65mg/kg, IV), diabetic CMN-treated (200 mg/kg, oral), diabetic PRP-treated (0.2 ml/kg, ip), and diabetic combined-treatment groups. Pancreatic specimens were arranged for biochemical analysis, processed for light and electron microscopic studies and were prepared for molecular analysis of the gene expression of insulin receptor-B (IR-B), insulin receptor substrate-1 (IRS-1) and PI3-kinase as a marker for phosphatidylinositol-3 kinase signalling pathway.

**Results:** Specimens of the diabetic group showed islet atrophy with apoptotic cellular changes, in addition to cellular depletion and vacuolar changes in some sections. Insulin immunostained sections showed weak immunoreactions. Electron microscopy showed small pyknotic beta cells' nuclei, numerous immature secretory granules, swelling of the mitochondria and endoplasmic reticulum and cytoplasmic rarefactions. In contrast, noticeable improvement was seen in monotherapy groups with a remarkable restoration in combination group. Noteworthy, potential islet cell regeneration was evident in PRP-treated group and became more prominent in the combined treatment group.

**Conclusion:** The individual use of each treatment showed satisfying results, regarding the islet structure and function, which qualify them to be used as an adjunctive therapy in the field of integrative medicine to manage type 1 DM. However, the use of both combined had a synergistic action, showed a better islet regeneration and might be a proper alternative for the burden of frequent insulin dosing and adjustment.



**Received:** 15 April 2021, **Accepted:** 31 May 2021

**Key Words:** Cinnamon, islet regeneration, platelet-rich plasma, ultrastructure.

**Corresponding Author:** Eman Mohamed Faruk Ahmed, MD, Department of Anatomy, Faculty of Medicine, Umm Al-Qura University, Saudi Arabia, Tel.: +20 10 9069 3901, E-mail: emkandel@uqu.edu.sa

**ISSN:** 1110-0559, Vol. 45, No. 3

## INTRODUCTION

Type 1 diabetes is a global health problem constituting about 5%-10% of Diabetes Mellitus all over the world<sup>[1]</sup>. Proper treatment requires precise dosing of exogenous insulin with frequent adjustment to control blood glucose levels within a normal range to minimize the risk of different complications. Frequent insulin dose adjustment and repeated glucose monitoring constitute a substantial burden that hurts the psychological wellbeing of diabetic individuals<sup>[1]</sup>. Another modality for a cure and mitigating the patient burden is based on the replacement of β-cells using either total pancreatic or partial islet cell transplantations however, the associated risk of invasive surgery, donor problems, and rejection complications have interfered with the wide-scale use of such approaches<sup>[2]</sup>. The innovation of safe and economic curative strategies that could enhance β-cell regeneration to alleviate patient suffering while improving the management of type 1 DM is a great demand that worth the collaboration of healthcare specialists.

Type 1 DM results from beta-cell mass loss due to a process of autoimmune destruction<sup>[3]</sup>. Hence, Streptozotocin (STZ) is widely used in experimental research to elicit type 1 DM due to its selective detrimental effect on pancreatic beta cells<sup>[4]</sup>.

Cinnamon (CMN), an ancient spice with various uses in the traditional kitchen, has got increasing attention in the research field due to its diverse biological activities. In both culture and animal-based studies, cinnamon showed strong anti-oxidative, anti-inflammatory, anticancer, and immunomodulatory effects. Also, it has been used to control blood glucose in diabetic patients<sup>[5]</sup>.

Platelet-rich plasma (PRP) is a biological blood product with higher concentrations of thrombocytes than those usually present in whole blood. Being a natural source of many growth factors and signalling molecules e.g. epidermal growth factor, insulin-like growth factor, VEGF that enhance neo-genesis and cellular differentiation, PRP has been used in different fields such as dermatology, wound healing, and cosmetic medicine<sup>[6]</sup> and has become an emerging promising strategy that caught insight in regenerative medicine over the last 20 years<sup>[7]</sup>.

In the current study, it is sought to investigate the islet cell protection that could be elicited by cinnamon and PRP either alone or in combination. Furthermore, the study evaluated the possible mechanisms entangled in such protection, at histo-biochemical, immunohistochemical, and molecular levels, in the current rat model of type DM.

## MATERIAL AND METHODS

### Animals

Fifty male Wistar albino rats, weighing about 200-230 g, were used in the current study. The animals were purchased from the breeding unit of the Egyptian Organization for Biological Products and Vaccines, VACSERA (Giza, Egypt), group-housed in an ambient temperate 26±2 °C, in a light-controlled room (12-hr light-dark cycles) and received commercial food and water ad libitum. Before experimentation, the animals were left without handling for one week for acclimatization and biological stabilization. The research protocol and all ethical issues regarding animal raising and experimentation of rats were approved and conducted following the Animal Care Guidelines and conforms with the recommendations of the National Institute of Health Guide for Care and Use of Laboratory Animals<sup>[8]</sup>.

### Chemicals and agents

- **Streptozotocin (STZ):** it was purchase from Sigma Aldrich, Egypt (CAS No. 18883-66-4, Sigma No. S0130), dissolved in sodium citrate buffer (0.1 M, pH 4.5) and freshly used within 5 minutes according to the manufacturer's instructions<sup>[9]</sup>.
- **Cinnamon water extract (CMN):** cinnamon bark was purchased from a local herbal plants market, Benha, Egypt. To prepare cinnamon water extract, five grams of cinnamon was dissolved in 100 ml water and boiled for 10 minutes at 45 °C, filtered, then stored in a refrigerator at 4 °C. The extract was freshly prepared every 2 days before use<sup>[10]</sup>. So, a final concentration of 50 mg/ml was obtained.
- **Activated Platelet-rich plasma (aPRP):** it was freshly prepared as mentioned later.

### Induction of Diabetes

Diabetes was elicited by a single intravenous (IV) injection of freshly prepared sterile STZ solution, at a dose of 65 mg/kg to overnight-fasted animals via tail vein<sup>[11]</sup>. After 3 days, the diabetic status of each animal was confirmed via tail-vein blood samples to determine fasting blood glucose level using a glucometer (Accu-Chek; Roche Diagnostics, Penzberg, Germany). On day 15 post-injection, the animals were overnight-fasted and blood glucose was estimated. Only animals with fasting blood glucose level of more than 250 mg/dl were included in the study<sup>[12]</sup>.

### **Preparation of aPRP and rat injection**

Fifteen male Wistar rats were used as a donor group to get PRP using the double centrifugation tube technique<sup>[13]</sup>. In brief, the rats were sacrificed by cervical dislocation after anaesthesia and the whole blood was obtained by cardiac puncture and collected into test tubes containing 3.8% sodium citrate anticoagulant at a blood/citrate ratio of 9/1. Then, the tubes were centrifuged at 400 ×g for 10 minutes. Three different density layers components were formed; the uppermost one composed of plasma and platelets; the lowermost one composed of red blood cells, and the middle one composed of a buffy coat of white blood cells. The plasma was taken with an automatic pipette carefully without affection of the middle buffy coat and taken to another tube that was re-centrifuged at 800 ×g for 10 min. This plasma centrifugation gave two parts: the upper one layer composed of platelet-poor plasma (PPP) and the lower layer composed of the platelet pellet. Most of the PPP was discarded while the platelet pellet was smoothly agitated and then put in phosphate-buffered saline (PBS) (1:1). The platelets count was more than 1,000,000/µl as they were counted by an automatic analyzer. Prior use, 10% CaCl<sub>2</sub> (0.8 ml PRP + 0.2 ml 10% CaCl<sub>2</sub>) was utilized to activate PRP.

### **Experimental design and animal grouping**

Fifteen rats were used for obtaining PRP and the other 35 animals were randomly assigned into:

- Control group: included 7 rats that received IV citrate buffer (0.1, pH 4.5; in an equal volume).
- Diabetic group: included 7 rats that received STZ only.
- Cinnamon-treated group: included 7 diabetic rats that received cinnamon, 200mg/kg, orally for 8 weeks<sup>[10]</sup>.
- PRP-treated group: included 7 diabetic rats that received activated PRP, 0.2 ml/kg body weight, intraperitoneal (ip) injection, once weekly for 2 months<sup>[14]</sup>.
- CMN+PRP-treated group: included 7 diabetic rats that received both agents in the same dose and duration as is the aforementioned groups.

### **Biochemical study**

#### **Assessment of the glycaemic metabolic state**

Initial blood sampling was done for measuring baseline fasting blood glucose (FBG) before grouping to ensure the normoglycemic state of the animals before experimentation. At the end of the experiment, blood samples were obtained via cardiac puncture under anaesthesia, centrifuged, stored at -20°C for later laboratory analysis for FBG and serum insulin levels. FBG analysis was done using the one-touch Accu-check glucometer (Roche Diagnostics, Manheim,

Germany) and its compatible blood glucose test strips. Serum insulin level was measured as previously described by Hiroyuk *et al.*<sup>[15]</sup> using a mouse insulin ELISA assay kit purchased from Bio-Diagnostic Company, Dokki, Giza, Egypt.

#### **Assessment of the pancreatic oxidant/antioxidant biomarkers**

Malondialdehyde (MDA) level, catalase (CAT), and superoxide dismutase (SOD) enzymatic activities were analyzed at room temperature in pancreatic homogenates prepared by grinding 0.5 mg of the pancreatic tissue sample in a mortar with liquid nitrogen and 4.5 mL of PBS. The ice was used to homogenize the mixture for 15 min by using an Ultra-Turrax homogenizer. The estimation of CAT and SOD activities was done by using commercially available kits according to the manufacturer's recommendations (Thermofisher Scientific, Cat. No. EIACATC for CAT and Cat No. EIASODC for SOD) as previously stated by Aebi<sup>[16]</sup> and Sun *et al.*<sup>[17]</sup> respectively. Results were written as millimole per minute per milligram tissue (mmol/min/mg tissue). While, lipid peroxidation biomarker; MDA, was measured according to the manufacturer's recommendations as described by Grotto *et al.*<sup>[18]</sup> using the commercial kits supplied by Abcam (Cat. No. ab118970). Results were written as nanomole per milligram tissue (nmol/mg tissue).

#### **Assessment of pancreatic inflammatory biomarkers**

Pancreatic tissue levels of tumour necrosis factor-alpha (TNF-α) and interleukin-6 (IL-6) were measured as previously demonstrated by Kalyuzhny<sup>[19]</sup> according to the manufacturer's instructions by the ELISA commercial kits (RayBiotech, USA, Cat No. ELHTNFA-CL-1 for TNF-α, Cat No. ELH-IL6-CL-1 for IL-6).

#### **RNA extraction and PCR for quantification of the gene expression level**

Pancreatic tissues were collected and stored at -70 oC for gene expression of insulin receptor-B (IR-B), insulin receptor substrate-1 (IRS-1) and PI3-kinase as a marker for phosphatidylinositol-3 kinase signalling pathway. Total RNA was extracted from pancreatic tissue homogenate using RNeasy purification reagent (Qiagen, Valencia, CA. Cat No./ID: 74104). cDNA was generated from 5µg of total RNA using RT reagent kit (Applied Biosystems, catalogue number 4306736). Real-time qPCR amplification and analysis were performed using SYBRs Green PCR Master Mix Reagents Kit (Applied biosystems, Catalog Number 4309155) as previously described by Iype *et al.*<sup>[20]</sup> and Applied Biosystem Instrument with software version 3.1 (StepOne™, USA). The qPCR assay with the primer sets was optimized at the annealing temperature of 60 oC (Table1).

**Table 1:** Primer sequences used for RT-qPCR amplification of genes

NM_017071.2 Rattus norvegicus insulin receptor (IR)	Forward primer 5'- GAGAGGAGAAACGGGAGACC -3' Reverse primer 5'- GACAGTCCTGGGAAGAGCAC-3' <a href="https://www.ncbi.nlm.nih.gov/tools/primer-blast/primertool.cgi?ctg_time=1613126683&amp;job_key=dX-qNLoIt6CQnrKbv_uWqcXgh5vo85yG6Q">https://www.ncbi.nlm.nih.gov/tools/primer-blast/primertool.cgi?ctg_time=1613126683&amp;job_key=dX-qNLoIt6CQnrKbv_uWqcXgh5vo85yG6Q</a>
NM_053481.2 Rattus norvegicus phosphatidyl inositol-4,5-bisphosphate 3-kinase (PI-3 kinase)	Forward primer 5'- GGAGTTCACCCTGTCCCTGTG -3' Reverse primer 5'- CATGCCGCCGTAAAATCAGG -3' <a href="https://www.ncbi.nlm.nih.gov/tools/primer-blast/primertool.cgi?ctg_time=1613128906&amp;job_key=9f8qtDkLNKMTnTGYPgVqkbjBjhr8B-Fag">https://www.ncbi.nlm.nih.gov/tools/primer-blast/primertool.cgi?ctg_time=1613128906&amp;job_key=9f8qtDkLNKMTnTGYPgVqkbjBjhr8B-Fag</a>
NM_012969.2 Rattus norvegicus insulin receptor substrate 1 (IRS-1)	Forward primer 5'- CCGGATACCGATGGCTTCTC -3' Reverse primer 5'- CCGCCACTTCTCTCGTTCT -3' <a href="https://www.ncbi.nlm.nih.gov/tools/primer-blast/primertool.cgi?ctg_time=1613129963&amp;job_key=1d8L4n5zc9tU5WngZIBN0h6bXOAziEf9Mg">https://www.ncbi.nlm.nih.gov/tools/primer-blast/primertool.cgi?ctg_time=1613129963&amp;job_key=1d8L4n5zc9tU5WngZIBN0h6bXOAziEf9Mg</a>
XR_598347.1 Glyceraldehyde-3-phosphate dehydrogenase (GAPDH)	Forward primer 5'- GATGCTGGTGTGAGTATGTCG -3' Forward primer 5'- GTGGTCAGGATGCATTGCTGA -3'

### Histological procedures

After blood sampling, the anesthetized animals were euthanized by cervical dislocation. Then, the abdominal cavities were opened, pancreata were dissected and rapidly removed, and fixed in 10% formal saline for later processing of paraffin sections. According to previously stated protocols, approximately five-micrometer sections were cut and were subjected to Hematoxylin and Eosin<sup>[21]</sup>, Mallory's trichrome stain<sup>[22]</sup>, and immunohistochemical staining using the peroxidase-labeled streptavidin-biotin method<sup>[23]</sup> for detection of insulin antibody. Mouse monoclonal insulin antibody (Catalog No. MA5-12037, Labvision Corporation, Fremont, CA, USA) was the primary antibody used herein. It was provided at 0.5–1.0 µg/mL dilution and incubated with the slide at room temperature for one hour. The sections were incubated with the primary antibody in PBS for one hour, followed by a reaction with biotinylated secondary antibody. After conjugation with streptavidin-biotin-peroxidase complex, 3,3-diaminobenzidine (DAB) was used as a chromogen and hematoxylin solution was used as a counterstain. The reaction gives brownish cytoplasmic discolouration. The positive control was the human pancreas with cytoplasmic staining of beta cells. Image acquisition was performed with digital microscope-camera (Leica Qwin 500, Leica, England) computer system.

For electron microscopy<sup>[24]</sup>, small pancreatic specimens (1 mm<sup>3</sup>) were fixed in 2.5–3 % buffered glutaraldehyde (pH 7.2 – 7.4) at 4 °C for 2 h, followed by post-fixation in 1% osmium tetroxide at 4 °C for thirty minutes, then dehydrated in serial dilutions of ethanol and finally embedded in epoxy resin (Epoxy Embedding Medium Kit; Sigma). Ultra-thin sections (70 nm) were cut using Leica Ultramicrotome, stained with uranyl acetate and lead citrate to be examined by JEM-2100 transmission electron microscope (TEM; JEOL, Tokyo, Japan) at the electron microscope unit in the Faculty of Agriculture, Mansoura University, Mansoura, Egypt.

### Histomorphometric study

Quantitative morphological image analysis was performed using the Leica Qwin computer system (Leica Qwin 500 MC, Leica, England) at the Faculty of Science,

Tanta University, Tanta, Egypt. It was composed of a camera (Model U-LHHG) and Imaging Software (Cell sense, Ver. 1.4.1). Islet profiles, in 10 randomly selected non-overlapping fields, were examined at different powers of magnifications in all the stained non-serially cut sections in all groups, to measure islet cell area, islet cell perimeter, number of islets per pancreatic section (numerical density of islets per section), number of cells per islets (cellular density/islet), number of insulin immunostained β-cells per islet (numerical density of β-cells/islet), and the area percent of Mallory-stained collagen fibers. The islet area and islet perimeter were estimated at high magnification. Almost rounded or nearly rounded islets were measured. Those with markedly distorted outlines were excluded to avoid the relative disproportionality between the perimeter and the area caused by the diverse shapes of islets. The number of islets was quantified at low magnification and was expressed as N/10 mm<sup>2</sup> of pancreatic tissue according to Noor *et al.*<sup>[25]</sup>. The cell number was counted at higher magnification using the counting tool to determine the total cellular density per islet and the β-cell density/islet, in particular. The cell count was estimated in 10 islet profiles per slide in each group.

### Statistical analysis

All data were recorded as a mean ± standard deviation (SD) for each parameter. Bartlett's test and Shapiro-Wilk test were used for the initial check of homogeneity and normality, respectively prior to the analysis. One-way analysis of variance (ANOVA) test was used followed by Tukey-Kramer as a post hoc test to measure statistical differences between groups. Differences were considered significant when the *P*-value < 0.05. Statistical analysis was carried out by using Graphpad Prism, Version 8.0 Software (GraphPad Software; San Diego, CA, USA).

## RESULT

### Mortality and clinical observations of the experimental animals

All the control and experimental animals survived throughout the study period with no deaths was observed among the animals. No clinical signs of significantly affected organ systems were noticed among the rats.

### Biochemical results

#### Effect of cinnamon and/or aPRP on the level of blood glucose and insulin

The effect of cinnamon and/or aPRP treatments on the levels of blood glucose and serum insulin was mentioned in (Table 2). It was seen that the level of blood glucose was significantly elevated ( $p < 0.05$ ) in the diabetic group when related to the control group. Remarkably, there was a significant reduction in the level of blood glucose in the diabetic groups treated with either cinnamon or aPRP ( $p < 0.05$ ) while, no significant difference was detected in the combination group when compared to the control animals.

More prominently to mention that this information was supported with the results of plasma insulin level (Table 2). There was a remarkable decrease ( $p < 0.05$ ) in the level of plasma insulin in the diabetic group when compared to the control group. Either cinnamon or aPRP treatment significantly increased ( $p < 0.05$ ) the plasma insulin level in diabetic group when compared with the diabetic untreated group, with normalization of the values in the combination group.

#### Effect of cinnamon and/or aPRP on the pancreatic oxidant/antioxidant biomarkers

Table 2 displayed a significant increment ( $p < 0.05$ ) in the pancreatic level of MDA in the diabetic group in relation to the healthy control group. In the cinnamon and/or aPRP-treated groups, the MDA level was significantly reduced ( $p < 0.05$ ) in comparison to the diabetic control group. The combination group showed normalization of MDA concentrations. On the other hand, the level of the enzymatic antioxidants (SOD and CAT) in the diabetic group was significantly decreased ( $p < 0.05$ ) comparing to control rats while significantly elevated ( $p < 0.05$ ) in the cinnamon and/or aPRP- treated groups when compared to the diabetic control group.

#### Effect of cinnamon and/or aPRP on the pancreatic inflammatory biomarkers

In diabetic control group, table 2 revealed a significant increase in the inflammatory biomarkers; TNF- $\alpha$  and IL-6 ( $P < 0.001$ ) when compared with the control group. Cinnamon and/or aPRP treatment showed a significant decrement ( $P < 0.001$ ) when compared to the diabetic control group with normalization of the values in combination group.

#### Quantification of insulin signalling proteins gene expressions by PCR

The insulin receptor (IR), insulin receptor substrate-1 (IRS-1), and PI-3 kinase (PI3k) gene expressions in the pancreatic tissues were illustrated (Figure 1). The graph showed a significant decrease in the relative gene expression of IR, IRS-1, and PI3k genes in diabetic control animals when compared to the healthy control rats. Either Cinnamon or PRP treatment exhibited a significant

elevation in the studied genes in comparison to the diabetic control group. Moreover, PRP treatment displayed a more significant therapeutic effect when compared to cinnamon. Whereas, normalization of the three studied genes was evident in the diabetic rats received combined treatment.

#### Effect of cinnamon and/or aPRP on the pancreatic histo-morphometric measurements

The data of the histomorphometric analysis of pancreatic tissue of control and treated diabetic rats are illustrated in (Table 3). There was a significant decrease ( $P < 0.001$ ) in the mean islet cell area and mean islet perimeter in the diabetic control group in relation to the healthy control group. Interestingly, the cinnamon and/or aPRP-treated groups showed a gradual significant restoration ( $P < 0.001$  for each) of the normal control values of the measured parameters, in relation to the diabetic control animals, which was significantly maximal ( $P < 0.001$ ) in the combined therapy group.

Regarding the mean cellular density (number of all endocrine cells) and the mean  $\beta$ -cells density (the number of insulin immunostained  $\beta$ -cells) per islet, there was a significant decrease ( $P < 0.001$ ) in both measured parameters in the diabetic control group compared to the healthy control, while in the cinnamon and/or aPRP-treated groups, there was a significant increase ( $P < 0.001$ ), compared to the diabetic control group, which was almost restored in the combined-therapy group. Furthermore, the mean number of islets was significantly affected ( $P < 0.001$ ) in the diabetic control group when compared to the healthy control, however, cinnamon and/or aPRP treatments significantly increased ( $P < 0.001$ ) the islet number that was significantly marked ( $P < 0.001$ ) in the combined therapy group.

Likewise, the mean area percent of collagen fibres deposition was more significantly increased ( $P < 0.001$ ) in the diabetic group than the control. Cinnamon and/or aPRP treatment significantly reduced ( $P < 0.001$ ) the collagen deposition, with almost restoration in the combined-therapy group.

#### Light microscopic findings

Hematoxylin and eosin-stained pancreatic sections of control animals showed a normal structural arrangement of the islet cells which appeared as a pale unstained area scattered among the deeply stained basophilic acini. The islet cells were arranged in cords or masses of cells with vesicular nuclei and acidophilic cytoplasm. The duct system appeared with normal epithelial lining (Figures 2A, 2B).

STZ injection in diabetic control group caused widening of the interacinar and interlobular connective tissue spaces with marked shrinkage of the islet cells associated with cellular changes in the form of pyknotic nuclei and hyperacidophilic cytoplasm. Islet vacuoles were seen both intracellular and intercellular due to cell shrinkage. Also, the islet cell distribution became less frequent throughout

the section. Some islet cells became degenerated with reduced cell number while others became depleted of cells (Figures 3A, 2B).

In CMN- and PRP-treated groups (Figures 4, 5 respectively), the pancreatic tissues of both groups showed remarkable improvement of the lobular architecture, restoration of the islet cell volume and distribution which was slightly less in CMN-treated animals.

Both combined therapy group showed a remarkable restoration of the pancreatic histoarchitecture. Islet cells restored their structural arrangement, size and distribution. One characteristic finding, in the pancreatic ducts of this animal group was the epithelial proliferation of the ductal lining cells that appeared as a stratified epithelium (Figures 6A, 6B). Also, some islets were noted linked to the nearby ones by a cord of cells, others appeared close to the proliferated duct system suggesting newly regenerated islets (Figure 6A). Surprisingly, the islets, in PRP-treated groups appeared more cellular suggesting the infiltration by potentially new formation of endocrine cells.

Mallory trichrome-stained sections of the control animals showed delicate collagen fibers deposition in between acini and interlobular spaces (Figure 7). The diabetic control group revealed massive deposition of blue-stained coarse collagen fibers interacinar, interlobular and around duct system. Extensive intra-islet accumulation of fibrous tissue strands was seen dividing the islets into cellular nests (Figure 8). CMN-, PRP-, and both combined groups show minimal fine collagen fibers deposition (Figures 9, 10, 11 respectively).

### **Immunohistochemical findings**

Immunostained pancreatic sections showed intense insulin immunoreactivity in the beta cells cytoplasm of the control rats (Figure 12). However, reduced immunoreaction was noticed in the islet cells of the diabetic control group (Figure 13). On the other hand, the treatment options showed strong cytoplasmic immunoexpression which was slightly less in the CMN-treated group (Figure 14) when compared to PRP-alone and both combined groups

(Figures 15, 16 respectively). Interestingly, immunolabelled cellular strands were seen connecting 2 disarrayed clusters of insulin immunostained islet cells indicating possible new formation of islets in the PRP-treated group (Figure 15).

### **Electron microscopic observations**

Electron microscopic examination of  $\beta$ -cells in control pancreatic islets revealed normal ultrastructure. The nuclei showed a homogenous distribution of fine granules (chromatin) with some peripheral condensation at the nuclear envelope. The mitochondria, rough endoplasmic reticulum (rER) appeared normal. Clear cell borders and intact intercellular junctions were evident. The secretory granules (SG) were equally distributed in the cytoplasm with an almost normal morphology. Each secretory granule was membrane-bound and showed a central spherical core with homogenous electron density surrounded by electron-lucent halos (Figure 17).

Electron micrographs of the  $\beta$ -cells of STZ-induced diabetic rats showed marked ultrastructural alterations. Most of the cells' nuclei appeared small and pyknotic denoting apoptotic changes. Some beta cells showed numerous immature secretory granules (with homogenous less electron-dense cores and no halos) (Figure 18A), while others revealed mature SG with a diminishment in granular content (Figure 18B). Rough endoplasmic reticulum were extensively dilated and swollen. Mitochondria were swollen with destroyed cristae and flocculent densities; cell borders were hazy with altered intercellular junctions. Signs of degenerated cytoplasm were prominent e.g. thinning of the cytoplasmic matrix, rarefaction, and vacuolization (Figure. 18B).

All treatment options in the different studied groups (Figures 19, 20, 21) showed remarkable improvement of the ultrastructural changes which was evident in the combined group (Figure 21). The cellular organelles appeared intact and SG were restored. However, minimally swollen round mitochondria and slightly less frequent SG were noted in the CMN-treated group (Figure 19).

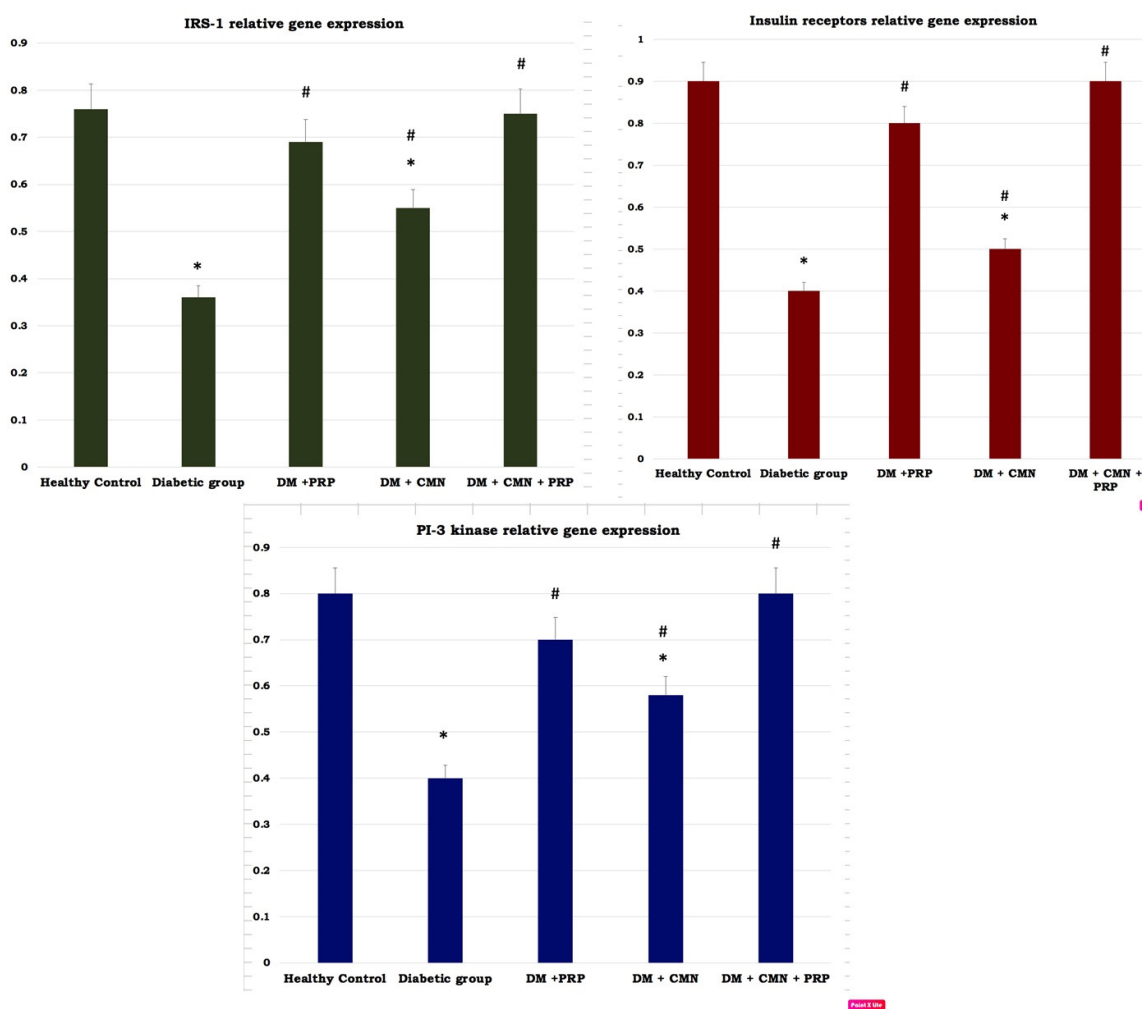


**Fig. 1:** mRNA expression profile of insulin signaling proteins in the pancreatic specimens of the studied groups. Gene expression of IR, IRS-1, and PI3k. \* Significant difference when compared to healthy control. # Significant difference when compared to diabetic control, using post hoc ANOVA,  $P < 0.05$ .

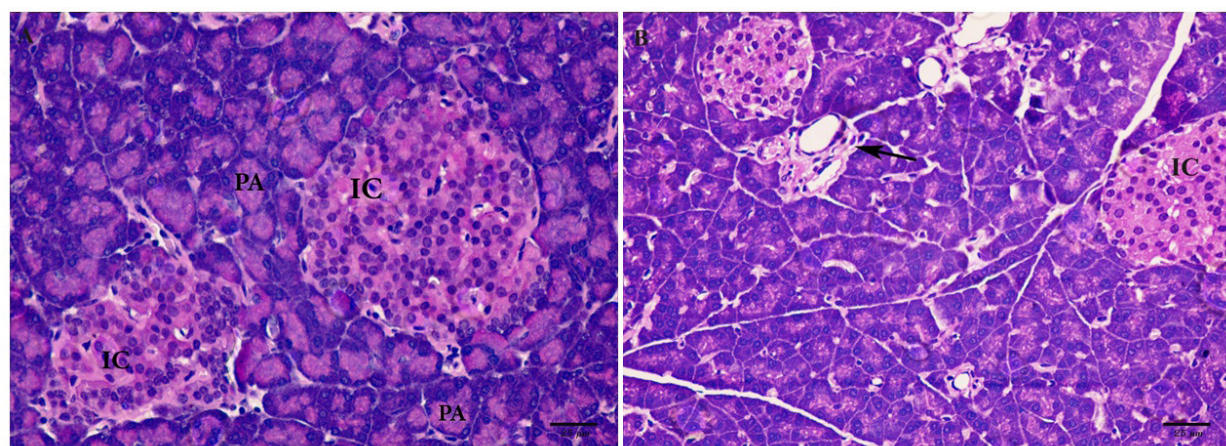


**Fig. 2:** H & E photomicrographs of the control group (A, B) showing normal structural arrangement of the islet cells (IC), pancreatic acini (PA), and pancreatic duct (arrow). Scale bar: 25  $\mu\text{m}$ .

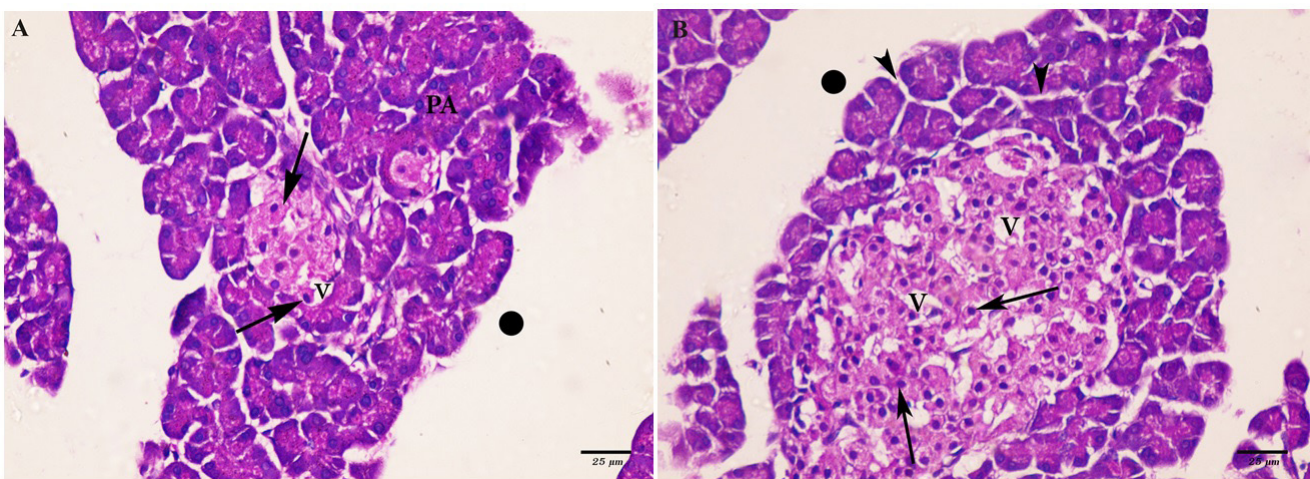


**Fig. 3:** H & E photomicrographs of the diabetic control group (A, B) revealing atrophic islet with cellular and intercellular vacuolations (V), cells (arrows) with pyknotic nuclei and hypereosinophilic cytoplasm. The interlobular (black circles) and interacinar spaces (arrowheads) are widened. Scale bar: 25  $\mu$ m.

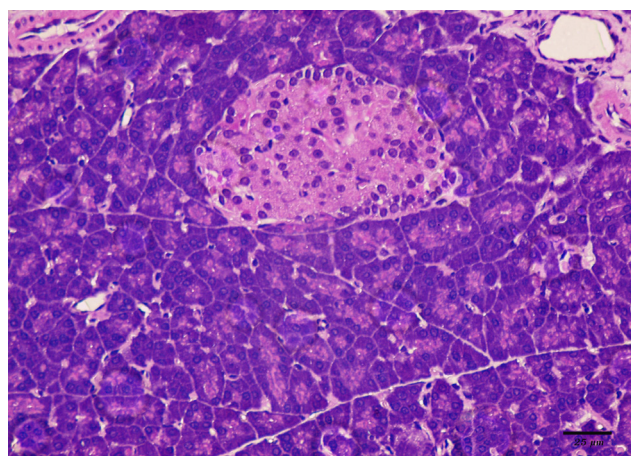


**Fig. 4:** H & E photomicrographs of the CMN-treated group showing almost normal microstructural organization of the islet cells (IC). Scale bar: 25  $\mu$ m.

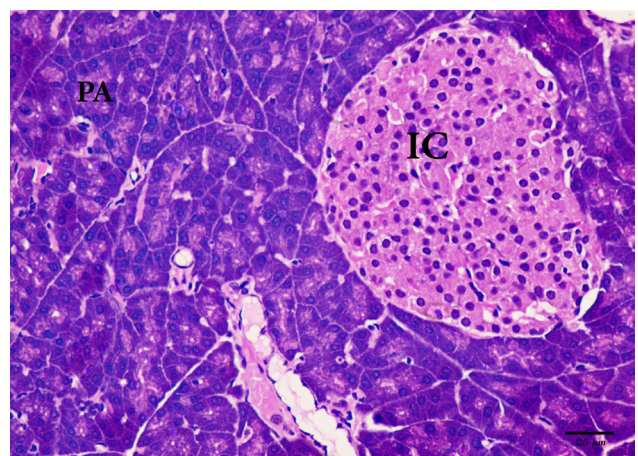


**Fig. 5:** H & E photomicrographs of the PRP-treated group showing normal histoarchitecture of the islet cells (IC). Heavy cellular population of the pancreatic islets (IC) was prominent. Scale bar: 25  $\mu$ m.

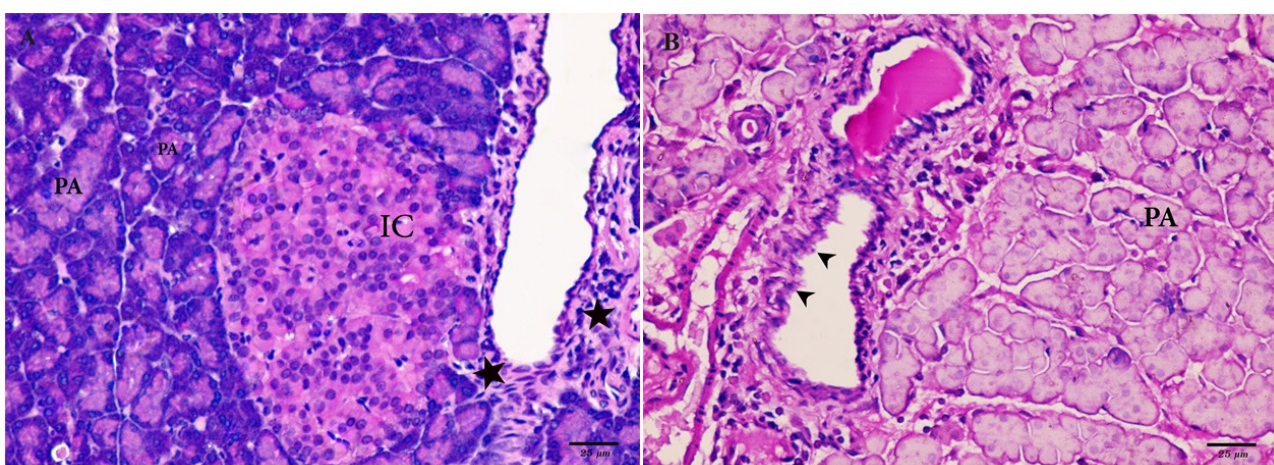


**Fig. 6:** H & E photomicrographs of the CMN+PRP-treated group (A, B) showing almost well organization of the cytoarchitecture of the pancreatic islets (IC). Notice, dense cellular population of the islets (IC). Also, ductal proliferation (stars) and epithelial stratification (arrowheads) were noted. Scale bar: 25  $\mu$ m.

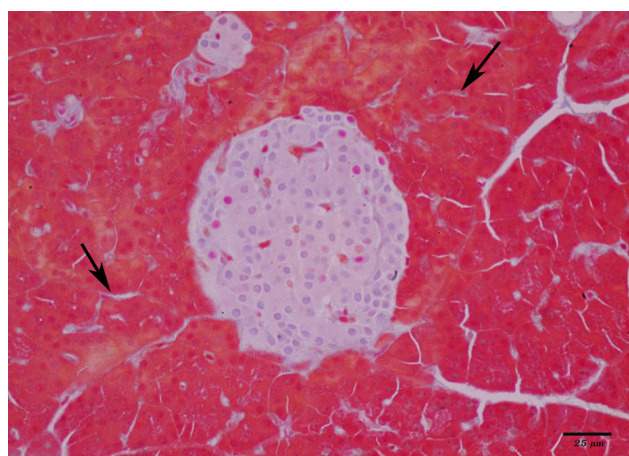


**Fig. 7:** Mallory trichrome stained photomicrographs of the control group showing delicate collagen fibers deposition in-between acini (arrows). Scale bar: 25  $\mu\text{m}$ .

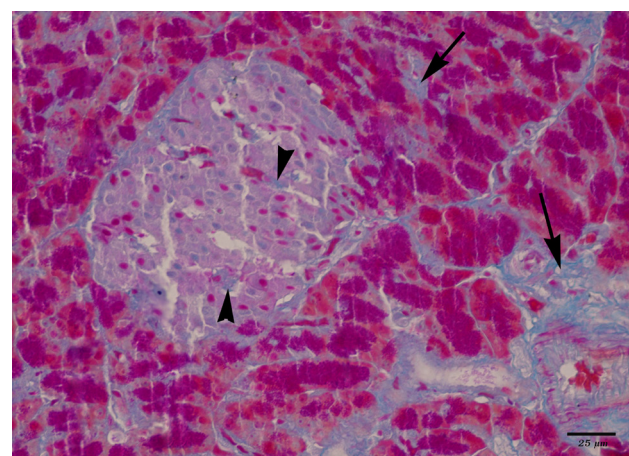


**Fig. 8:** Mallory trichrome stained photomicrographs of the diabetic control group showing extensive deposition of blue-stained coarse collagen fibers interacinar, interlobular and around duct system (arrows). Extensive intra-islet accumulation of fibrous tissue strands are seen (arrowheads). Scale bar: 25  $\mu\text{m}$ .

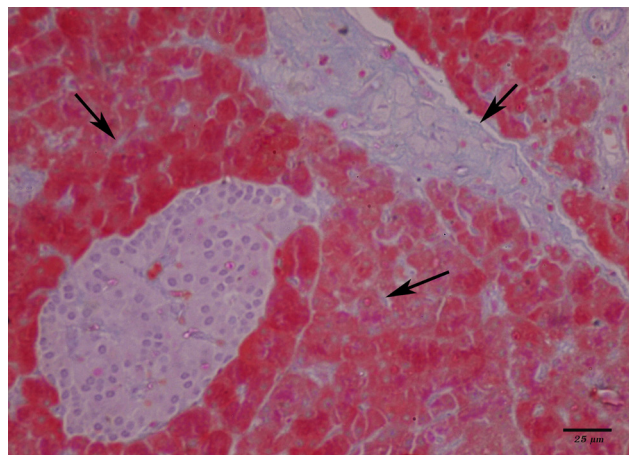


**Fig. 9:** Mallory trichrome stained photomicrographs of the CMN- treated group showing minimal fine collagen fibers distribution. Scale bar: 25  $\mu\text{m}$ .

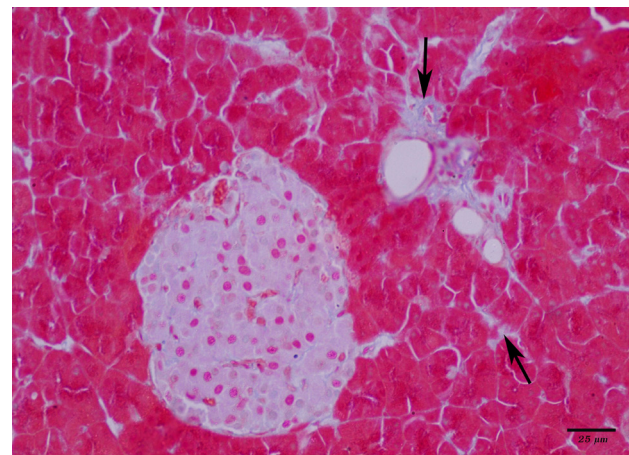


**Fig. 10:** Mallory trichrome stained photomicrographs of the PRP-treated group showing scarce fine collagen fibers deposition. Scale bar = 25  $\mu\text{m}$  scale.

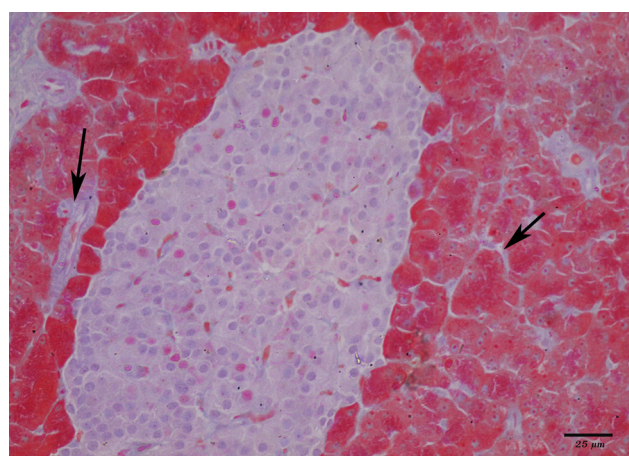


**Fig. 11:** Mallory trichrome stained photomicrographs of the combined group showing minimal fine collagen fibers distribution. Scale bar = 25  $\mu\text{m}$ .

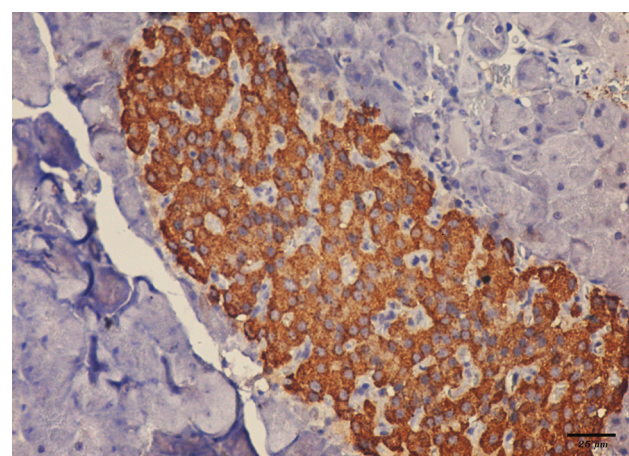


**Fig. 12:** Insulin immunostained pancreatic sections of the control islets cells showing cytoplasmic brown discoloration (arrows) denoting beta cells with positive immunoreaction, surrounded by a peripheral zone of negative alpha cells (arrowheads). Scale bar: 25  $\mu\text{m}$ .

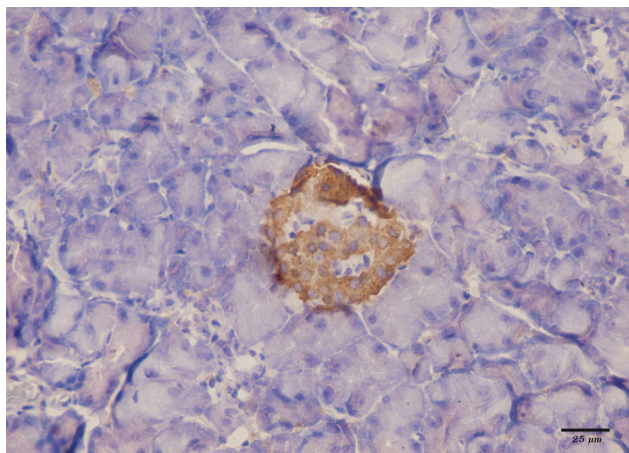


**Fig. 13:** Insulin immunostained pancreatic sections of the diabetic control group showing atrophic pancreatic islet with reduced intensity of the  $\beta$ -cells immune-labelling. Scale bar: 25  $\mu\text{m}$ .

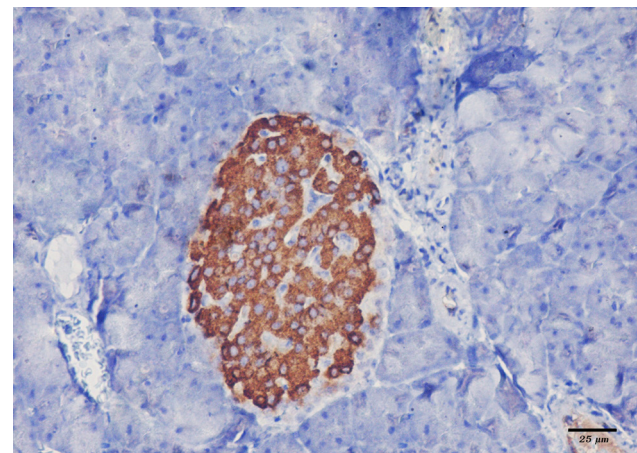


**Fig. 14:** Insulin immunostained pancreatic sections of the CMN-treated group less strong islet immunoreaction. Scale bar: 25  $\mu\text{m}$ .

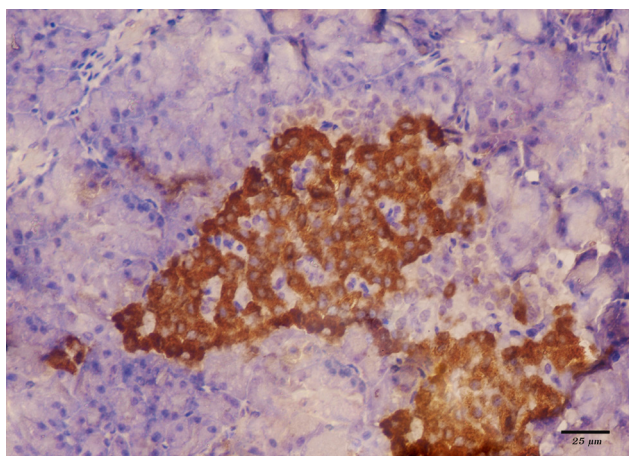


**Fig. 15:** Insulin immunostained pancreatic sections of the PRP-treated group showing islet cells with strong positive immunoreaction. Notice, immunolabelled creeping cellular strands (double-arrows) are seen communicating between 2 disarrayed clusters of immunostained islets. Scale bar: 25  $\mu\text{m}$ .

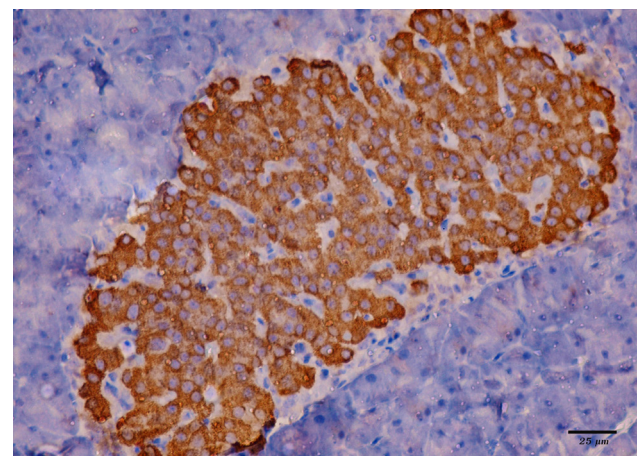


**Fig. 16:** Insulin immunostained pancreatic sections of the CNM+PRP-treated groups showing the islet cells with strong positive insulin immunolabelled  $\beta$ -cells. Scale bar = 25  $\mu\text{m}$

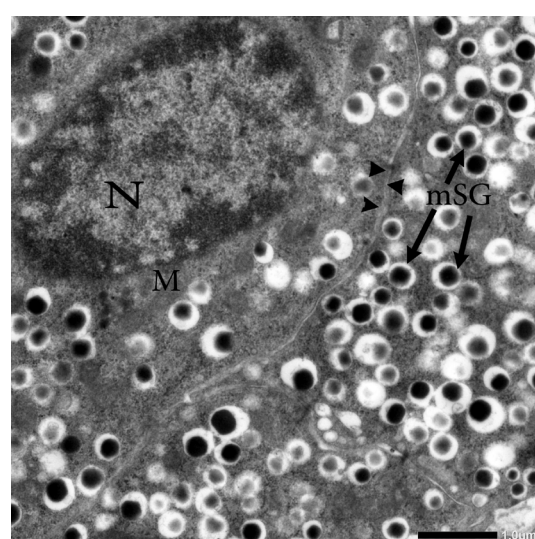


**Fig. 17:** EM photomicrographs of beta cells of the control group showing homogenous nuclear (N) chromatin distribution with some peripheral nuclear condensation. Mature secretory granules (mSG) appears in normal size and number and shows central spherical core surrounded by electron lucent halos. The cell organelles appears with normal shape, the clear cell borders are clear (arrowheads). Scale bar: 1  $\mu\text{m}$ .

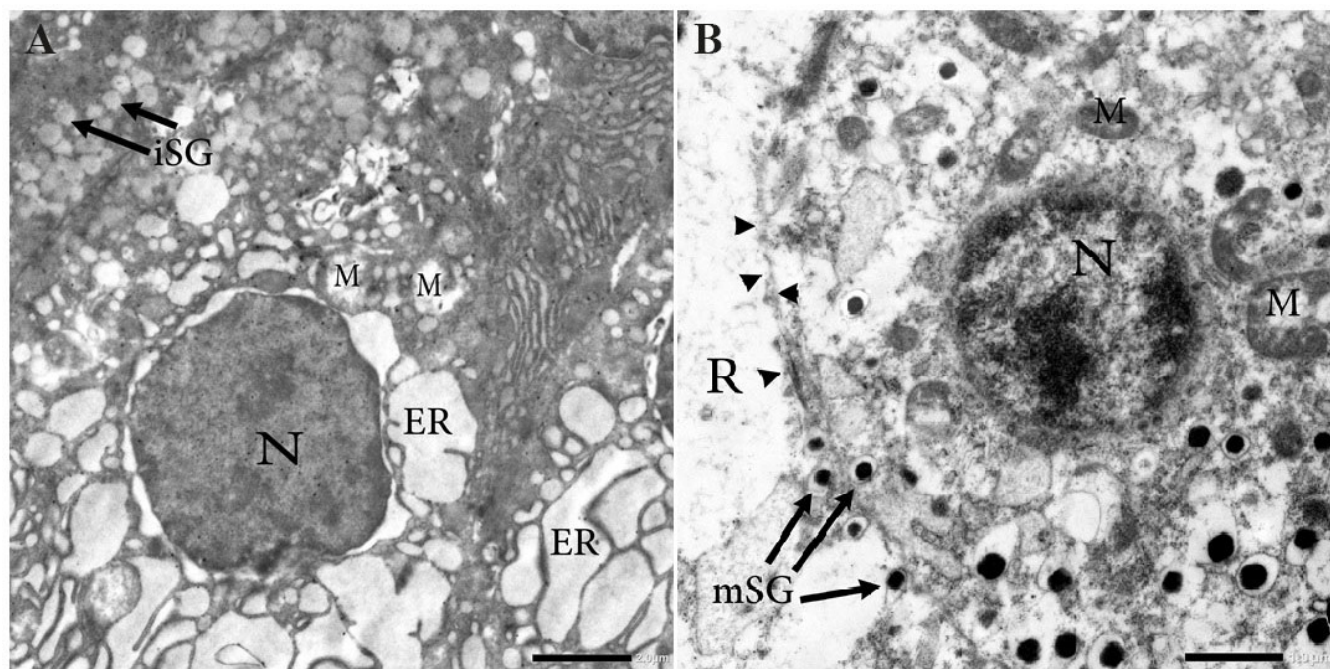


**Fig. 18:** EM photomicrographs of beta cells of the diabetic control group (A, B) showing small condensed pyknotic nuclei (N), swollen mitochondria (M) with destroyed cristae and dilated endoplasmic reticulum (ER). Also, numerous immature secretory granules (iSG) with less electron dense core are seen. Other  $\beta$ -cells show mature secretory granules (mSG) with reduced number and size. Cytoplasmic rarefaction (R) and vacuolization are noticed. Cell boundaries are hazy and not clear (arrowheads). Scale bar: a: 2 $\mu$ m; b: 1 $\mu$ m.

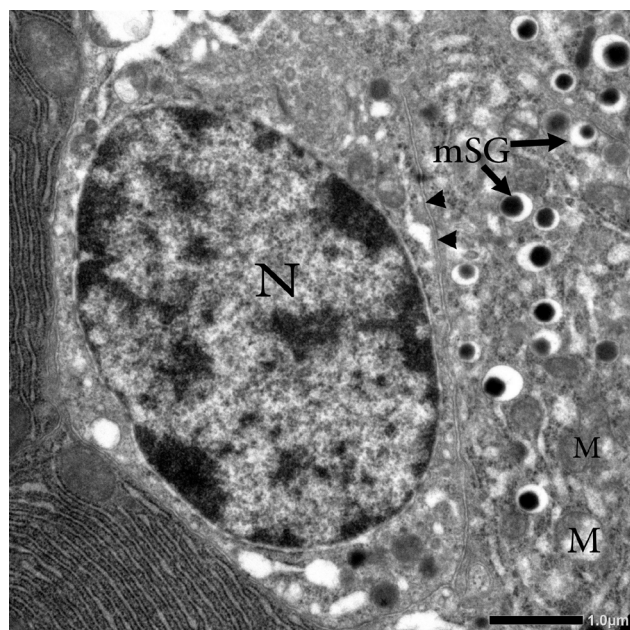


**Fig. 19:** EM photomicrographs of beta cells of the CMN-treated group showing obvious improvement of the cellular organelles, however Mitochondria (M) are slightly swollen and secretory granules (mSG) are slightly reduced in number. Scale bar: 1 $\mu$ m.

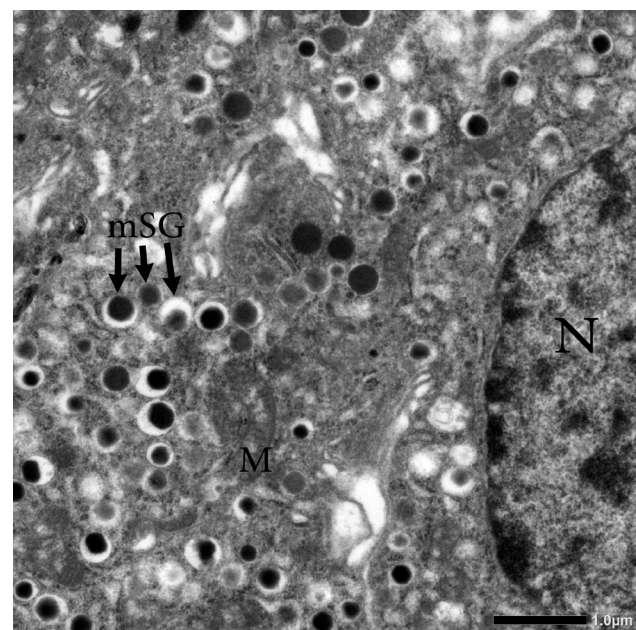


**Fig. 20:** EM photomicrographs of beta cells of the PRP-treated group showing striking improvement of the cellular organelles. Scale bar: 1 $\mu$ m.

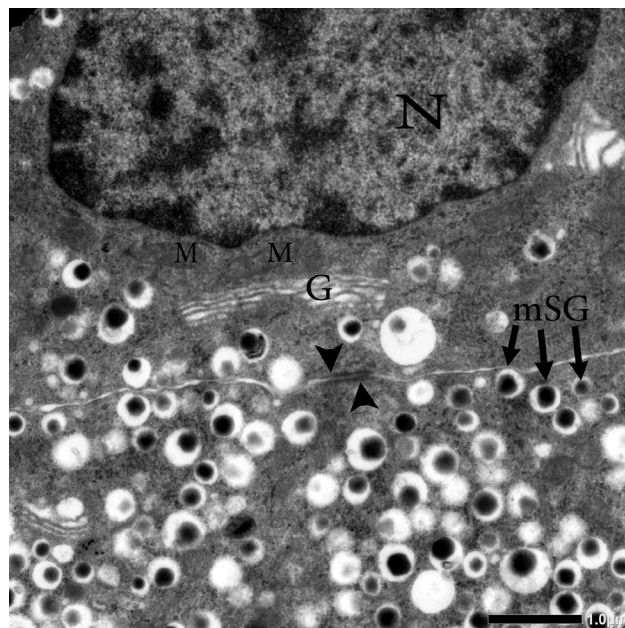


**Fig. 21:** EM photomicrographs of beta cells of the CMN+PRP-treated groups showing marvelous restoration of the ultrastructure of the cell organelles. Scale bar: 1 $\mu$ m.

**Table 2:** Effect of cinnamon and/or aPRP on blood glucose, serum insulin levels, pancreatic inflammatory biomarkers, and oxidant/antioxidant biomarkers in treated and untreated diabetic rats

Parameters	Control	Diabetic	DM+cinnamon	DM+aPRP	DM+cinnamon+aPRP
Blood glucose (md/dl)	124.1 $\pm$ 1.18	310.2 $\pm$ 1.35 <sup>a</sup>	162.2 $\pm$ 2.32 <sup>ab</sup>	150.9 $\pm$ 1.16 <sup>abc</sup>	126.2 $\pm$ 1.23 <sup>bcd</sup>
Serum insulin(U/mL)	7.26 $\pm$ 2.26	2.65 $\pm$ 1.14 <sup>a</sup>	4.31 $\pm$ 1.02 <sup>ab</sup>	5.11 $\pm$ 1.10 <sup>abc</sup>	6.96 $\pm$ 1.02 <sup>bcd</sup>
SOD (mmol/min/mg)	159.9 $\pm$ 3.00	75.4 $\pm$ 3.60 <sup>a</sup>	127.2 $\pm$ 1.82 <sup>ab</sup>	145.2 $\pm$ 1.35 <sup>abc</sup>	157.1 $\pm$ 2.09 <sup>bcd</sup>
CAT (mmol/min/mg)	109.0 $\pm$ 2.60	74.3 $\pm$ 1.5 <sup>a</sup>	83.1 $\pm$ 1.36 <sup>ab</sup>	95.4 $\pm$ 1.27 <sup>abc</sup>	105.6 $\pm$ 2.81 <sup>bcd</sup>
MDA ( $\mu$ mol/mL)	12.62 $\pm$ 1.24	26.2 $\pm$ 2.71 <sup>a</sup>	16.3 $\pm$ 1.63 <sup>ab</sup>	15.2 $\pm$ 2.10 <sup>ab</sup>	13.01 $\pm$ 1.21 <sup>bcd</sup>
TNF- $\alpha$ (pg/100 $\mu$ g protein)	12.31 $\pm$ 1.63	25.02 $\pm$ 2.08 <sup>a</sup>	14.21 $\pm$ 1.73 <sup>ab</sup>	13.71 $\pm$ 3.24 <sup>ab</sup>	12.77 $\pm$ 1.23 <sup>bcd</sup>
IL-6 (pg/100 $\mu$ g protein)	6.11 $\pm$ 1.01	11.07 $\pm$ 1.05 <sup>a</sup>	8.12 $\pm$ 1.02 <sup>ab</sup>	7.13 $\pm$ 2.03 <sup>abc</sup>	6.51 $\pm$ 1.52 <sup>bcd</sup>

All values are presented as mean  $\pm$  SD. a significant vs control group, b significant vs diabetic group, c significant vs diabetic+ cinnamon group and d significant vs diabetic+ aPRP within a row, by ordinary ANOVA or Welch's ANOVA test followed by Tukey's test and Dunnett's T3 test post-hoc multiple comparisons tests, respectively, at  $P$ -value  $< 0.05$ . Abbreviations; DM, diabetes; aPRP, activated platelet rich plasma; SOD, superoxide dismutase; CAT, catalase; MDA, malondialdehyde

**Table 3:** Effect of cinnamon and/or aPRP on islet area (mm<sup>2</sup>), Islet cell perimeter (um), Number of cells per islet, islet number (N/10 mm<sup>2</sup>), mean area percent of collagen fibers, and number of  $\beta$ -cells/islet in diabetic group

Parameters	Control	Diabetic	DM+cinnamon	DM+aPRP	DM+cinnamon+aPRP
Islet cell area (mm <sup>2</sup> )	0.01695 $\pm$ 0.001	0.00587 $\pm$ 0.0006 <sup>a</sup>	0.01283 $\pm$ 0.0009 <sup>ab</sup>	0.01431 $\pm$ 0.0007 <sup>abc</sup>	0.01662 $\pm$ 0.0004 <sup>abcd</sup>
Islet cell perimeter (um)	507.83 $\pm$ 35.33	219.6 $\pm$ 21.1 <sup>a</sup>	356.7 $\pm$ 11.74 <sup>ab</sup>	407.21 $\pm$ 24.1 <sup>abc</sup>	509.61 $\pm$ 39.2 <sup>abcd</sup>
Number of cells per islet	253.23 $\pm$ 17.12	89.17 $\pm$ 9.14 <sup>a</sup>	230.16 $\pm$ 12.19 <sup>ab</sup>	245.89 $\pm$ 15.1 <sup>abc</sup>	255.01 $\pm$ 19.05 <sup>bcd</sup>
Islet number (N/10 mm <sup>2</sup> )	14.63 $\pm$ 0.61	5.43 $\pm$ 0.31 <sup>a</sup>	10.54 $\pm$ 0.41 <sup>ab</sup>	12.91 $\pm$ 0.11 <sup>abc</sup>	14.1 $\pm$ 0.01 <sup>abcd</sup>
Area percent of collagen fibers	3.12 $\pm$ 1.02	16.14 $\pm$ 0.34 <sup>a</sup>	4.23 $\pm$ 1.12 <sup>ab</sup>	5.09 $\pm$ 1.21 <sup>abc</sup>	3.02 $\pm$ 1.02 <sup>bcd</sup>
Number of insulin immunostained $\beta$ -cells/islet	189.92 $\pm$ 9.11	66.87 $\pm$ 1.21 <sup>a</sup>	172.62 $\pm$ 3.01 <sup>ab</sup>	184.41 $\pm$ 6.21 <sup>abc</sup>	191.25 $\pm$ 2.02 <sup>bcd</sup>

All values are presented as mean $\pm$ SD. a significant vs control group, b significant vs diabetic group, c significant vs diabetic+ cinnamon group and d significant vs diabetic+ aPRP within a row, by ordinary ANOVA or Welch's ANOVA test followed by Tukey's test and Dunnett's T3 test post-hoc multiple comparisons tests, respectively, at  $P$ -value  $< 0.05$ . Abbreviations; DM, diabetes; aPRP, activated platelet rich plasma

## DISCUSSION

The current study investigated the effect of 2 natural resources either alone or in combination, the ancient spice (cinnamon) and the blood product (platelet-rich plasma) on the pancreatic structure and function of type 1 diabetes rat model. Although their potency curative leverage has been reported in the literature, their concomitant administration herein was the first such attempt, to the best of the authors' knowledge. Moreover, the pancreatic ultrastructure in rats treated by CMN and PRP has lesser attention in the literary report so, the study analyzed the obtained data in correlation with the biochemical, histological, immunohistochemical, and ultrastructural viewpoints along with quantification of mRNA gene expression for the insulin signalling proteins encoding genes (IR-B, IRS-1, and PI3k) by RT-qPCR.

The findings of the current work showed a synergistic action of the 2 agents when co-administered together, in the present rat model of STZ-induced DM. The H & E findings showed that STZ injection in the diabetic control rats caused a remarkable shrinkage and structural disarrangement of the islet cells. Such histological observation was corroborated by the histomorphometric results that showed a significant reduction in the mean islet area, perimeter and mean number of  $\beta$ -cells per islet when compared to the control findings. In agreement, Yi *et al.*<sup>[26]</sup> reported atrophic changes in the islet cells of STZ-treated mice.

The histological results were supported and explained by the ultrastructural observations of beta cells of the same group that revealed small pyknotic nuclei, dilation of the endoplasmic reticulum which explained the cytoplasmic vacuolation in H and E results, degenerated swollen mitochondria, and disruption of the cell boundary and membrane junctions. Also, some beta cells showed numerous immature secretory granules while others showed mature ones with diminished granular content and number. When correlating the biochemical analysis of the pancreatic tissue homogenates, the diabetic control group showed a significant elevation of tissue MDA, coincided with a significant decrease in CAT and SOD denoting a status of cellular oxidative stress that could explain the mitochondrial ballooning and ER dilation in EM as demonstrated by Ahn *et al.*<sup>[27]</sup>. They concluded an ER stress induced by STZ in mice pancreas with subsequent apoptosis. Also, we reported a significant increase in the pancreatic tissue levels of inflammatory mediators; TNF and IL-6. In agreement, Fathy and Drees<sup>[28]</sup> recorded a significant elevation of MDA, TNF, and IL-6 in the pancreatic tissue of diabetic rats.

All these ultrastructure changes supported by the biochemical results of tissue homogenate explained the diabetogenic mechanism of STZ as demonstrated by<sup>[4,29]</sup> who reported beta-cell membrane stress-mediated disintegrity with altered properties and a major mitochondrial role with energy store depletion precipitated by STZ injection. Given the aforementioned affected cellular organelles are actively participating in insulin synthesis<sup>[30]</sup>, hence

interfering with insulin synthesis and release. These findings explained the significant decrease in both the mean number of insulin immunostained  $\beta$ -cells and serum insulin level in the immunohistochemical and biochemical results, respectively. Noteworthy, the increased number of immature granules in the  $\beta$ -cell cytoplasm led us to suggest a hyper-function of the remaining beta cells to compensate for the decreased serum insulin level. In addition, the results displayed a significant reduction in the mRNA expression of all the studied insulin signalling proteins (IR-B, IRS-1, and PI3k) in the diabetic control group when compared to the healthy control animals. Similarly, Balbaa *et al.*<sup>[31]</sup> and Gouda *et al.*<sup>[32]</sup> reported a downregulation in the gene expression level of insulin and insulin receptors. Even, the sole downregulation of IR levels could interrupt the subsequent cascade involved in insulin signalling such as tyrosine phosphorylation of IR and IRS-1 as well as the associated P85/PI3K activity with IRS-1 in response to insulin<sup>[33]</sup>.

Taken together, we suggested that the reduced insulin secretion in diabetic rats was due to  $\beta$ -cells inflammatory and oxidative stress that led to ultrastructural changes of the cellular organelles involved in insulin synthesis and secretion and led to altered insulin expression at gene and protein levels, as demonstrated by mRNA expression quantification and immunohistochemical observations respectively. This suggestion was asserted by Balbaa *et al.*<sup>[31]</sup> who discussed that the oxidant/antioxidant imbalance and increased release of proinflammatory cytokines such as TNF- $\alpha$  could impair insulin signalling pathway and gene expressions

Interpretation of the Mallory stained pancreatic sections revealed excess fibrous tissue deposition within the islets cells of the untreated diabetic rats. Similarly, Zechner *et al.*<sup>[34]</sup> reported excess collagen I deposition in a mice model of STZ-induced diabetes. Lee *et al.*<sup>[35]</sup> attributed these islet fibrotic changes to the activation of the intra-islet pancreatic stellate cells (PSCs) that deposited excess extracellular matrix proteins (ECM). Diabetes activates PSCs via a renin angiotensin-mediated mechanism and hyperglycemia-induced oxidative stress. Also, the interlobular and inter-acinar collagen deposition could be explained by the decreased insulin level as postulated by Altay<sup>[36]</sup> who suggested a negative impact of insulinopenia on pancreatic acini and stroma.

Regarding the cinnamon- and PRP-treated group, the H & E findings showed a notable restoration of the pancreatic histoarchitecture. In accordance, previous studies<sup>[37,38]</sup> reported a protective effect of cinnamon and PRP on the pancreatic structure and function in diabetic rat models. In parallel, the electron microscopic results explained the improvement in the islet histoarchitecture. The cytoplasm and nuclei restored their usual density, cell borders became clear, mitochondria and endoplasmic reticulum became almost normal although still slightly swollen and rounded in the cinnamon-treated group. The secretory granules restored their content and number

denoting restoration of the insulin synthesis and release as asserted by the significant increase of the mean number of insulin immunostained  $\beta$ -cells and serum insulin level. In harmony, the mRNA expression levels of IR-B, IRS-1, and PI3k, in both groups, showed a significant increase when compared to the diabetic group with the excellence of PRP over cinnamon treatments. In agreement, Karimi Fard *et al.*<sup>[39]</sup> recorded a significant effect for cinnamon on the GLUT4 and IR gene expression in diabetic rat adipose tissue. Also, Nemati *et al.*<sup>[40]</sup> reported a significant increase in pancreatic gene expression of insulin in PRP-treated diabetic rats.

On the opposite, the reversal of the oxidative stress and the proinflammatory micro milieu of the pancreas by CMN and or PRP might improve its structure and secretory function. Actually, the biochemical findings displayed a reestablishment of the normal pancreatic levels of MDP, CAT, SOD, TNF, and IL-6 in both groups with superiority of PRP treatment. These findings coincided with Zarin *et al.*<sup>[38]</sup> who showed significantly decreased MDA concentrations and increased activity of SOD in the pancreas of diabetic rats. Also, Mirmiranpour *et al.*<sup>[41]</sup> reported an increase in the enzymatic antioxidant activity in type 2 diabetic patients when treated by cinnamon. Prior experimental studies revealed a magic antioxidant capability for PRP in various diseased organs; in testicular ischemia/reperfusion<sup>[42]</sup>, cardiotoxicity<sup>[43]</sup>, and osteoarthritis<sup>[44]</sup>. Therefore, the antioxidant and anti-inflammatory capacity introduced by cinnamon and PRP could be a reasonable explanation for the improved histological, immunohistochemical and gene expression findings.

More interesting, seemingly newly regenerated islet cells were observed in the PRP-treated group as evident by the immunohistochemical observation of small scattered, disarrayed insulin immunostained islets connected by crawling immunolabelled cellular strands. In fact, platelets secrete myriads of growth factors that have vital roles in the development of the pancreas and the proliferation of beta cells to maintain normal islet function. These signals such as insulin-like and platelet-derived growth factors have been evaluated as emerging remedies in regenerative medicine such as treatment of diabetes as they can stimulate proliferation of  $\beta$ -cells<sup>[45]</sup>. Platelet-rich plasma has concentrations of thrombocytes greater than those in whole blood<sup>[6]</sup> and its injection to diabetic rats, in the current work, restored islet volume, distribution, and cellular replenishment in H & E observations as confirmed by the histomorphometry of the islet profiles which showed a significant increase when compared to the CMN group. In addition, the mean  $\beta$ -cell number per islet was significantly higher in PRP-treated animals that denoted heavily populated cellular islets by putatively new endocrine cells. Hence, the herein result proposed that the released growth factors from the activated PRP might stimulate the proliferative capacity of these cells and enhance the gene expression of insulin signalling proteins.

In the authors' opinion, the subsidence of the diabetic state with subsequent inactivation of the PSCs and restoration of the resting conditions, as demonstrated formerly, could explain the minimal delicate collagen deposition in Mallory Trichrome-stained sections of the CMN- and PRP-treated groups. This was in contradiction with Bynigeri *et al.*<sup>[46]</sup> who reported a set of cytokines and platelet-derived growth factors that were involved in the activation of quiescent pancreatic stellate cells (PSCs) and excess extracellular matrix (ECM) production. Such discrepancy could be addressed by a former analytical study of PRP constituents<sup>[47]</sup>. They reported the presence of agonistic and antagonistic growth factors, in PRP, whose predominance depends on the centrifugation method used. Furthermore, the reversal of the diabetic state and the reduced glucose level could have an effect added to the antagonistic growth factors that finally limit inflammation, fibrosis, and enhance regeneration<sup>[48]</sup>.

Turning to the combined-treatment group, marked improvement in the pancreatic cytoarchitecture was obtained with almost normalization of the islet cell morphometric parameters. These observations were asserted by the electron microscopic findings that showed a remarkable improvement of the ultrastructural changes denoted by the recovery of the cellular organelles and secretory granules. One interesting H & E finding, in this animal group, was the proliferation of the ductal lining cells. Also, some islet cells were seen in close proximity to the proliferated ducts. These observations could suggest a possible emerging role of the ductal progenitors in neo-genesis of islet cells under the effect of CMN/PRP combination, as demonstrated by Arutyunyan *et al.*<sup>[49]</sup>, who mentioned the existence of pancreatic ductal stem cells that could differentiate into  $\beta$ -cells. Further methods such as markers of proliferation and differentiation are warranted for the assertion of the entangling of the pancreatic ducts in the neo-genesis of islet cells.

The current observation emphasized our suggestion that there were certain platelet growth factors that could, in harmony with cinnamon, stimulate the differentiation of the ductal stem cells in the injured pancreas. This notion was in agreement with Qian *et al.*<sup>[50]</sup> who reported a stem cell differentiation enhanced by PRP during regeneration of the musculoskeletal system. Noteworthy, the normalization of the gene expression in this animal group together with the eminent insulin immunoexpression indicated an optimum insulin secretion and release, at gene and protein levels, that was reflected in the normalization of serum insulin level and hence the significant decrease in glucose levels. These observations pointed to a synergistic effect elicited by the simultaneous implementation of both agents that could be explained by a further additive effect of the antioxidant and anti-inflammatory capacities obtained when both combined as confirmed by the obvious improvement of the tissue biomarkers of inflammation and oxidative stress.

The current study findings recorded possible  $\beta$ -cell proliferation and or ductal cells transdifferentiation as

suggested mechanisms of the regenerative capacity of PRP that might be synergized by CMN combination, as confirmed by Crisci *et al.*<sup>[51]</sup> who explored a variety of suggested mechanisms by which the platelet-derived growth factors exerted their tissue repair effects. One mechanism was the control of recruitment, proliferation, and differentiation of cells involved in the regenerative process, proliferation and adherence of stem cell progenitors, regulation of angiogenesis in injured tissue via a controlled release of proangiogenic and antiangiogenic factors. Also, remodeling and restoration of the extracellular matrix. Finally, they reported a regenerative action via the achievement of an apoptosis/cell survival balance, which is the main fate of tissue injury.

#### AUTHORS' CONTRIBUTION

Almost all the authors have contributed equally to the current work. Usama Fouad has contributed to the idea of the study, study design, monitoring the practical experiment, prepared the manuscript draft, data interpretation, and writing discussion. Eman Faruk has contributed to photographing the light microscopic slides, writing figures legend, statistical data analysis, and interpretation, writing discussion and revision of the drafted manuscript. Ahmed Morsi has contributed to experimental design and animal grouping, critical analysis and interpretation of the collected data, writing light and electron microscopic results, writing discussion, and revising the manuscript for type editing. Hanan Fouad performed the biochemical analysis of blood and tissue samples, gene expression study, analysis of data, writing discussion, and revising the manuscript for type editing. All authors have read and approved the submitted manuscript.

#### ACKNOWLEDGMENT

The authors would like to thank the Deanship of Scientific Research at Umm Al-Qura University for supporting this work by Grant Code: (22UQU4331391DSR03).

#### CONCLUSION

Briefly, STZ injection in the current rat model of type 1 DM exerted drastic histo-biochemical, immunohistochemical, and ultrastructural changes alongside the downregulation of the gene expressions of insulin signalling proteins. Cinnamon and platelet-rich plasma (PRP) are economic and safe natural resources that were attempted concomitantly, in the present study and showed surprising results in reversing the disturbed parameters induced by STZ. Interestingly, the activated PRP displayed a potential regenerative capacity of the islet cells as denoted by the immunohistochemical observations and the heavy population of the depleted diabetic islets by putatively new endocrine cells in H & E findings. In addition, their combination with cinnamon exhibited a possible transdifferentiation capacity of the ductal progenitor cells into new  $\beta$ -cells. Furthermore, the anti-inflammatory and antioxidant activities of both agents were added when given simultaneously. The obtained results

enforce the researchers to encourage the new concept of regenerative and integrative medicine and to use CMN and or PRP as a complementary therapy combined with the traditional medications. Moreover, it was shown that their combination achieved a better result than individual use of each that makes them a qualified, cheap, and safe potential approach to substitute the frequent insulin injection and dosing during the management of type 1 DM patients.

#### CONFLICT OF INTERESTS

There are no conflicts of interest.

#### REFERENCES

1. Duke DC, Barry S, Wagner D V, *et al.* Distal technologies and type 1 diabetes management. Lancet Diabetes Endocrinol. 2018; 6:143–156.
2. Vantyghem M-C, de Koning EJP, Pattou F, Rickels MR. Advances in  $\beta$ -cell replacement therapy for the treatment of type 1 diabetes. Lancet. 2019; 394:1274–1285.
3. Tomita T. Apoptosis of pancreatic  $\beta$ -cells in type 1 diabetes. Bosn J basic Med Sci. 2017; 17(3):183-193.
4. Wu J, Yan L-J. Streptozotocin-induced type 1 diabetes in rodents as a model for studying mitochondrial mechanisms of diabetic  $\beta$  cell glucotoxicity. Diabetes, Metab Syndr Obes targets Ther. 2015; 8:181.
5. Ribeiro-Santos R, Andrade M, Madella D, *et al.* Revisiting an ancient spice with medicinal purposes: Cinnamon. Trends Food Sci Technol. 2017; 62:154–169.
6. Alves R, Grimalt R. A review of platelet-rich plasma: history, biology, mechanism of action, and classification. Ski appendage Disord. 2018; 4:18–24.
7. Alsousou J, Harrison P. Platelet-rich plasma in regenerative medicine. In: Gresele P, Kleiman N, Lopez J, Page C. (eds) Platelets in thrombotic and non-thrombotic disorders, 1st ed. 2017; Springer, Cham, New York, USA, pp 1403–1416.
8. NIH. Guide for the Care and Use of Laboratory Animals. 8th ed. 2011. National Academies Press (US). pp 220.
9. Kuloglu T, Aydin S. Immunohistochemical expressions of adropin and inducible nitric oxide synthase in renal tissues of rats with streptozotocin-induced experimental diabetes. Biotech Histochem. 2014; 89:104–110.
10. Kouame K, Peter AI, Akang EN, *et al.* Effect of long-term administration of Cinnamomum cassia silver nanoparticles on organs (kidneys and liver) of Sprague-Dawley rats. Turkish J Biol. 2018; 42:498–505.
11. Wang-Fischer Y, Garyantes T. Improving the Reliability and Utility of Streptozotocin-Induced Rat Diabetic Model. J Diabetes Res. 2018; 2018:8054073.

12. Sharafeldin K, Rizvi MR. Effect of traditional plant medicines (*Cinnamomum zeylanicum* and *Syzygium cumini*) on oxidative stress and insulin resistance in streptozotocin-induced diabetic rats. *J Basic Appl Zool.* 2015; 72:126–134.
13. Pazzini JM, Nardi AB De, Huppes RR, et al. Method to obtain platelet-rich plasma from rabbits (*Oryctolagus cuniculus*). *Pesqui Veterinária Bras.* 2016; 36:39–44.
14. Dehghani F, Aboutalebi H, Esmaeilpour T, et al. Effect of platelet-rich plasma (PRP) on ovarian structures in cyclophosphamide-induced ovarian failure in female rats: a stereological study. *Toxicol Mech Methods.* 2018; 28:653–659.
15. Hiroyuki S, Masaaki S, Yoshio T, et al. An enzyme immunoassay system for measurement of serum insulin. *Mol Immunol.* 1980; 17:377–381.
16. Aebi H. Catalase in vitro. *Methods Enzymol.* 1984; 105:121–126.
17. Sun YI, Oberley LW, Li Y. A simple method for clinical assay of superoxide dismutase. *Clin Chem.* 1988; 34:497–500.
18. Grotto D, Maria LS, Valentini J, et al. Importance of the lipid peroxidation biomarkers and methodological aspects for malondialdehyde quantification. *Quim Nova.* 2009; 32:169–174.
19. Kalyuzhny EA. Handbook of ELISPOT: methods and protocols. *Methods Mol Biol.* 2<sup>nd</sup> ed. 2005; 302:1–323.
20. Iype T, Francis J, Garmey JC, et al. Mechanism of insulin gene regulation by the pancreatic transcription factor Pdx-1: application of pre-mRNA analysis and chromatin immunoprecipitation to assess formation of functional transcriptional complexes. *J Biol Chem.* 2005; 280:16798–16807.
21. Bancroft JD, Lyton C. The Hematoxylins and Eosin. In: Suvarna SK, Bancroft JD, Lyton C (eds) *Bancroft's theory and practice of histological techniques*, 8<sup>th</sup> ed, 2018; Ed. pp 126–138.
22. Bancroft JD, Layton C. The Hematoxylins and Eosin /Connective and other mesenchymal tissues with their stains. In: Suvarna KS, Layton C, Bancroft JD (eds) *Bancroft's theory and practice of histological techniques E-Book*, 8<sup>th</sup> ed. 2019; Elsevier Health Sciences.
23. Kiernan JA. Immunohistochemistry. In: Kiernan J (ed) *Histological and histochemical methods. Theory and practice*, 4<sup>th</sup> ed. 2015; Scion Publishing Ltd, pp 454–490.
24. Anthony WE, John SW. Transmission electron microscopy. In: Suvarna SK, Bancroft JD, Lyton C (eds) *Bancroft's theory and practice of histological techniques E-Book*, 8<sup>th</sup> ed. 2018; Elsevier Health Sciences, pp 434–475.
25. Noor A, Gunasekaran S, Vijayalakshmi MA. Improvement of Insulin Secretion and Pancreatic  $\beta$ -cell Function in Streptozotocin-induced Diabetic Rats Treated with Aloe vera Extract. *Pharmacognosy Res.* 2017; 9:S99–S104.
26. Yi J-K, Ryoo Z-Y, Ha J-J, et al. Beneficial effects of 6-shogaol on hyperglycemia, islet morphology and apoptosis in some tissues of streptozotocin-induced diabetic mice. *Diabetol Metab Syndr.* 2019; 11:1–13.
27. Ahn C, An B-S, Jeung E-B. Streptozotocin induces endoplasmic reticulum stress and apoptosis via disruption of calcium homeostasis in mouse pancreas. *Mol Cell Endocrinol.* 2015; 412:302–308.
28. Fathy SM, Drees EA. Protective effects of Egyptian cloudy apple juice and apple peel extract on lipid peroxidation, antioxidant enzymes and inflammatory status in diabetic rat pancreas. *BMC Complement Altern Med.* 2015; 16:1–14.
29. Lee S-H, Han Y-M, Min B-H, Park I-S. Cytoprotective effects of polyenoylphosphatidylcholine (PPC) on  $\beta$ -cells during diabetic induction by streptozotocin. *J Histochem Cytochem.* 2003; 51:1005–1015.
30. Li DT, Habtemichael EN, Julca O, et al. Focus: Organelles: GLUT4 Storage Vesicles: Specialized Organelles for Regulated Trafficking. *Yale J Biol Med.* 2019; 92:453.
31. Balbaa M, El-Zeftawy M, Ghareeb D, et al. Nigella sativa relieves the altered insulin receptor signaling in streptozotocin-induced diabetic rats fed with a high-fat diet. *Oxid Med Cell Longev.* 2016; 2016:16.
32. Gouda W, Hafiz NA, Mageed L, et al. Effects of nanocurcumin on gene expression of insulin and insulin receptor. *Bull Natl Res Cent.* 2019; 43:1–10.
33. Boucher J, Kleinridders A, Kahn CR. Insulin receptor signaling in normal and insulin-resistant states. *Cold Spring Harb Perspect Biol.* 2014; 6:a009191–a009191.
34. Zechner D, Knapp N, Bobrowski A, et al. Diabetes increases pancreatic fibrosis during chronic inflammation. *Exp Biol Med.* 2014; 239:670–676.
35. Lee E, Ryu GR, Ko S-H, et al. A role of pancreatic stellate cells in islet fibrosis and  $\beta$ -cell dysfunction in type 2 diabetes mellitus. *Biochem Biophys Res Commun.* 2017; 485:328–334.
36. Altay M. Which factors determine exocrine pancreatic dysfunction in diabetes mellitus? *World J Gastroenterol.* 2019; 25(22): 2699–2705.
37. Hassanen N. Protective Effect of cinnamon, clove and ginger spicces or their essential oils on oxidative stress of streptozotocin-induced diabetic rats. *J Agric Sci.* 2010; 18:137–154.

38. Zarin M, Karbalaei N, Keshtgar S, Nemati M. Platelet-rich plasma improves impaired glucose hemostasis, disrupted insulin secretion, and pancreatic oxidative stress in streptozotocin-induced diabetic rat. *Growth Factors*. 2019; 37:226-237.
39. Karimi Fard M, Khajehlandi A, Mohammadi A. The Effect of Swimming Training and Cinnamon Consumption on the Gene Expression of GLUT4 and Insulin Receptor in the Brown Adipose Tissue of Diabetic Rats. *Gene, Cell Tissue*. 2021; 8 (1):6.
40. Nemati M, Karbalaei N, Mokarram P, Dehghani F. Effects of platelet-rich plasma on the pancreatic islet survival and function, islet transplantation outcome and pancreatic pdx1 and insulin gene expression in streptozotocin-induced diabetic rats. *Growth Factors*. 2021; 1-15.
41. Mirmiranpour H, Huseini HF, Derakhshanian H, et al. Effects of probiotic, cinnamon, and synbiotic supplementation on glycemic control and antioxidant status in people with type 2 diabetes; a randomized, double-blind, placebo-controlled study. *J Diabetes Metab Disord*. 2019;19(1):53-60.
42. Sekerci CA, Tanidir Y, Sener TE, et al. Effects of platelet-rich plasma against experimental ischemia/reperfusion injury in rat testis. *J Pediatr Urol*. 2017; 13:317.e1-317.e9.
43. Zaki SM, Algaleel WAA, Imam RA, Abdelmoaty MM. Mesenchymal stem cells pretreated with platelet-rich plasma modulate doxorubicin-induced cardiotoxicity. *Hum Exp Toxicol*. 2019; 38:857–874.
44. Ragab GH, Halfaya FM, Ahmed OM, et al. Platelet-Rich Plasma Ameliorates Monosodium Iodoacetate-Induced Ankle Osteoarthritis in the Rat Model via Suppression of Inflammation and Oxidative Stress. *Evidence-Based Complement Altern Med*. 2021; 2021:13.
45. Aamodt KI, Powers AC. Signals in the pancreatic islet microenvironment influence β-cell proliferation. *Diabetes, Obes Metab*. 2017; 19:124-136.
46. Bynigeri RR, Jakkampudi A, Jangala R, et al. Pancreatic stellate cell: Pandora's box for pancreatic disease biology. *World J Gastroenterol*. 2017; 23:382.
47. Pochini A de C, Antonioli E, Bucci DZ, et al. Analysis of cytokine profile and growth factors in platelet-rich plasma obtained by open systems and commercial columns. *Einstein (Sao Paulo)*, 2016; 14(3):391-397.
48. El-Sharkawy H, Kantarcı A, Deady J, et al. Platelet-rich plasma: growth factors and pro-and anti-inflammatory properties. *J Periodontol*. 2007; 78:661-669.
49. Arutyunyan I V, Fatkhudinov TK, Makarov A V, et al. Regenerative medicine of pancreatic islets. *World J Gastroenterol*. 2020; 26(22): 2948–2966.
50. Qian Y, Han Q, Chen W, et al. Platelet-rich plasma derived growth factors contribute to stem cell differentiation in musculoskeletal regeneration. *Front Chem*. 2017; 5:89.
51. Crisci A, De Crescenzo U, Crisci M. Platelet-rich concentrates (L-PRF, PRP) in tissue regeneration: Control of apoptosis and interactions with regenerative cells. *J Clin Mol Med*. 2018; 1:1-2.

## الملخص العربي

# حماية البنكرياس الناتجة عن تركيبة البلازمـا الغـنية بالصفائح الدموـية والـقرفة في نـموذج الفـئران المصـابة بـداء السـكري من النوع الأول: هل هي حـقبة جـديدة في تـجـديـد خـلايا الجـزـيرـية للـبنـكريـاس وـالـتـعبـيرـاتـ الجـينـيـة لـلـأـنسـولـينـ؟

اسـامـه فـؤـاد اـحمد اـبرـاهـيمـ، اـحمد عـبد الرـحـمـن مـرسـىـ، حـنـان فـؤـادـ، إـيمـان مـحمد فـارـوقـ،<sup>٠</sup>

قـسـم التـشـريـح - كـلـيـة الطـب - جـامـعـة بنـهاـ

قـسـم الـهـسـتوـلـوـجـياـ - كـلـيـة الطـب - جـامـعـة الفـيـوـم - جـامـعـة بنـهاـ

قـسـم الـكـمـيـاء الـحـيـوـيـة - كـلـيـة الطـب - جـامـعـة الـقـاهـرـة

قـسـم التـشـريـح - كـلـيـة الطـب - جـامـعـة اـم القرـىـ

**المقدمة:** يعتبر استحداث التجدد لجزر لانجرهانز هو مطلب كبير يستحق اهتمام الباحثين ومقدمي الرعاية الصحية لتجنب مخاطر زراعة الخلايا في مرضي السكر من النوع الاول.

**الهدف:** تقييم القدرة التجددية والعلاجية لكلا من القرفة والبلازمـا الغـنية بالصفائح الدموـية إما بمفردها أو مجتمعة على تحسين التركيب الدقيق للبنكرياس وانتظام المسارات الخاصة بافراز الأنسولين في الفـئـران المصـابة بـداء السـكري المستحدث بمادة الاستربـوتـوزـوـتوـسيـنـ.

**مواد وطرق البحث:** تم استخدام خمسة عشر ذكوراً من الجرذان البيضاء للحصول على البلازمـا الغـنية بالصفائح الدموـية، واستخدمـتـ الـ ٣٥ جـرـذاـ المـتـبـقـيـةـ كالـاتـيـ: مـجمـوعـة ضـابـطـةـ، المـجمـوعـةـ المـسـتـحدـثـ بهاـ مـرضـ السـكـرـ بـمـادـةـ الاستـربـوتـوزـوـتوـسيـنـ (٦٥ مـجمـ / كـجمـ، وـريـدـ)، المـجمـوعـةـ المعـالـجـةـ بـالـقـرـفـةـ (٢٠٠ مـجمـ / كـجمـ، عنـ طـرـيقـ الفـمـ)، المـجمـوعـةـ المعـالـجـةـ البـلـازـمـاـ الغـنـيـةـ بـالـصـفـائـحـ الدـمـوـيـةـ (٢٠٠ مـلـ / كـغـ، حقـنـ بـرـيتـونـيـ)، المـجمـوعـةـ المعـالـجـةـ بـالـأـثـنـيـنـ مـعـاـ. تم تجهيز وتحضـيرـ اـنسـجـةـ الـبـنـكريـاسـ لـلـتـحلـيلـ الـكـيـمـيـائـيـ الـحـيـوـيـ، لـلـفـحـصـ الـمـجـهـرـيـ الـضـوـئـيـ وـالـإـلـكـتـرـوـنـيـ، كـمـاـ تـمـ تـحـضـيرـهاـ لـلـتـحلـيلـ الـجـزـيـئـيـ لـفـحـصـ الـجـيـنـاتـ الـخـاصـةـ بـمـسـتـقـبـلاتـ الـأـنسـولـينـ (IR-B)ـ وـ(PI3-kinaseـ).

**النتائج:** أظهرت عينات المجموعة المستحدث بها مرض السكر ضمور في جزر لانجرهانز مع وجود مؤشرات لموت الخلايا المبرمج، بالإضافة إلى ندرة الخلايا وظهور فجوات سيتوبلازمية في بعض العينات. أظهرت العينات المحضرة بالصبغة المناعية ضعف في التفاعل المناعي للأنسولين. كما أظهر الفحص بالمجهر الإلكتروني لخلايا بيتا وجود نوى صغيرة داكنة اللون، كثير من الحبيبات الإفرازية غير الناضجة، وانتفاخ الميتوكوندريا والشبكة الإندوبلازمية بالإضافة إلى تغيرات في السيتوبلازم. على النقيض، تبين تحسن ملحوظ في المجموعتين المعالجتين بكل مادة بمفردها مع تحسن أفضل في المجموعة التي عولجت بالاثنتين معا. وتتجدر الإشارة إلى أن احتمال تجدد خلايا الجزر كان واضحاً في المجموعة المعالجة بالبلازمـاـ الغـنـيـةـ بـالـصـفـائـحـ الدـمـوـيـةـ وأـصـبـحـ أـكـثـرـ بـرـوزـاـ فيـ المـجمـوعـةـ الـتـىـ عـولـجـتـ بـهـمـاـ مـعـاـ.

**الخلاصة:** أظهر الاستخدام الفردي لكل علاج على حده نتائج مرضية، فيما يتعلق بتركيب ووظيفة خلايا لانجرهانز، مما يؤهلهما للاستخدام كعلاج مساعد في مجال الطب التكاملـيـ للـتعـامـلـ معـ مـرضـ السـكـرـ بـمـادـةـ النـوعـ الأولـ. ومع ذلكـ، فـانـ استخدامـ كـلـ الـخـيـارـينـ مـعـاـ لهـ تـأـثـيرـ تـأـزـرـيـ، وأـظـهـرـ تـجـدـداـ أـفـضـلـ لـخـلـاـيـاـ جـزـرـ لـانـجـرـهـانـزـ وـقدـ يـكـونـ بـدـيـلـاـ منـاسـبـاـ لـلـحقـنـ الدـائـمـ لـلـأـنسـولـينـ وـالـتـعـديـلـ المـتـكـرـرـ لـلـجـرـعـاتـ.